



Bubbleless aerated-biological activated carbon as a superior process for drinking water treatment in rural areas

Mengjie Liu ^{a,b}, Nigel Graham ^c, Lei Xu ^a, Kai Zhang ^a, Wenzheng Yu ^{a,*}

^a State Key Laboratory of Environmental Aquatic Chemistry, Key Laboratory of Drinking Water Science and Technology, Research Center for Eco-Environmental Sciences, Chinese Academy of Sciences, Beijing, 100085, China

^b University of Chinese Academy of Sciences, Beijing, 100049, China

^c Department of Civil and Environmental Engineering, Imperial College London, South Kensington Campus, London, SW7 2AZ, United Kingdom

ARTICLE INFO

Keywords:

Biological activated carbon (bac)
Bubbleless aeration
Natural organic matter (nom)
DBP formation
Rural drinking water

ABSTRACT

Drinking water supply in rural areas remains a substantial challenge due to complex natural, technical and economic conditions. To provide safe and affordable drinking water to all, as targeted in the UN Sustainable Development Goals (2030 Agenda), low-cost, efficient water treatment processes suitable for rural areas need to be developed. In this study, a bubbleless aeration BAC (termed ABAC) process is proposed and evaluated, involving the incorporation of a hollow fiber membrane (HFM) assembly within a slow-rate BAC filter, to provide dissolved oxygen (DO) throughout the BAC filter and an increased DOM removal efficiency. The results showed that after a 210-day period of operation, the ABAC increased the DOC removal by 54%, and decreased the disinfection byproduct formation potential (DBPFP) by 41%, compared to a comparable BAC filter without aeration (termed NBAC). The elevated DO ($> 4 \text{ mg/L}$) not only reduced secreted extracellular polymer, but also modified the microbial community with a stronger degradation ability. The HFM-based aeration showed comparable performance to 3 mg/L pre-ozonation, and the DOC removal efficiency was four times greater than that of a conventional coagulation process. The proposed ABAC treatment, with its various advantages (e.g., high stability, avoidance of chemicals, ease of operation and maintenance), is well-suited to be integrated as a pre-fabricated device, for decentralized drinking water systems in rural areas.

1. Introduction

Providing adequate and safe drinking water is a service with immeasurable economic and health benefits (UNGA 2001). Investment in drinking water services has brought safely managed drinking water services to two billion people worldwide in the last two decades (WHO 2023). Despite this progress, two billion people still do not have access to safe and reliable drinking water, and poor drinking water systems remain a major challenge, particularly in rural areas and small municipalities, where drinking water is usually pumped directly from wells or obtained from natural water sources without adequate treatment (Bei et al., 2019; Wang et al., 2021b).

Due to complex natural, technical and economic conditions (e.g., terrain, materials, cost and labor issues), large-scale, centralized drinking water supply systems used in large, urban areas cannot be applied effectively to small-scale communities in rural areas (Song et al., 2020). Interest in the use of slow biofiltration processes in rural drinking water

supply projects has increased in recent years, because of their relative simplicity, low operating cost and easy maintenance (Song et al., 2020). Riverbank filtration, for example, accounts for 6.5 percent and 16 percent of the total amount of drinking water produced in the Netherlands and Germany, respectively (Bertelkamp et al., 2014; Gillefalk et al., 2018). Slow sand filtration shares similar principles with riverbank filtration, using sand or anthracite instead of an aquifer as the filter material (Bauer et al., 2011). Such engineered biofiltration is more versatile in practical applications. However, long residence times and low removal rates are the two major drawbacks of current biofiltration process. For example, a riverbank filtration process with a 36-hour residence time showed only ~33% DOC removal efficiency (Zhao et al., 2022). Shortening the residence time leads to inadequate biodegradation, as demonstrated by a previous study which showed ~11% DOC removal for a sand filtration with a residence time of 45 min (Hallé et al., 2009).

Since biodegradation is the primary mechanism for biofiltration,

* Corresponding author.

E-mail address: wzyu@rcees.ac.cn (W. Yu).

increasing biomass and increasing biodegradation efficiency are two factors to enhance the performance of biological filtration. Granular activated carbon (GAC), with its high porosity, can provide large surface area for organics absorption and a substrate for growth of microbial biofilms. Biofiltration using GAC as filter material has been widely applied to remove a variety of contaminants, such as biodegradable and recalcitrant dissolved organic matter (DOM), ammonia, emerging micro-pollutants, flavor and odor compounds, from water (Reungoat et al., 2011; Rattier et al., 2012; Jantaraksen et al., 2020; Rui et al., 2020; Zhang et al., 2021). Another limitation of slow biofiltration is the insufficient dissolved oxygen (DO) within the fixed bed. It has been reported that the progressive consumption of DO resulted in anoxic conditions and a poor degradation efficiency in the middle and downstream regions of the BAC process (Zheng et al., 2010; Chuang and Mitch 2017; Munz et al., 2019). Moreover, Chuang et al. found that saturation of DO in the influent did not prevent DO deficiency in the middle of the BAC filter (Chuang and Mitch 2017). A laboratory-scale river-bank filtration test suggested that a more effective removal under aerobic conditions (9–13%) as compared to anoxic conditions (6–10%) (Baumgarten et al., 2011). In order to elevate the DO concentration, some studies have adopted an up-flow configuration to improve the oxygen availability (Lu et al., 2013; Rui et al., 2020). Other studies have treated the influent with ozone or pure oxygen prior to the BAC process (Reungoat et al., 2011; Phungsai et al., 2018; Chang et al., 2022), but aeration is energy intensive, and the use of ozone significantly increases the operational cost. More importantly, aeration of the influent does not successfully address the problem of oxygen deficiency within the BAC system. (Chuang and Mitch 2017) found that although pre-ozone increased the influent DO concentrations close to saturation, the DO declined to 0.3 – 0.6 mg/L upon BAC treatment at 15 min empty bed contact time.

Based on the above discussion, a simple, low-cost approach to providing oxygen throughout the whole BAC process is necessary for the sustainable application of the BAC process in rural areas. In this study, “bubbleless aeration” was used to distributed pressurized air into the

BAC process by means of a hollow fiber membrane (HFM) module (Zhang et al., 2022). Compared to bubble aeration, HFM-based aeration has the advantage of uniform mass transfer, low supply pressure, and a low operational cost (Aybar et al., 2014; Hou et al., 2019; Zhang et al., 2022). The performance of bubbleless aeration BAC (termed ABAC) and non-aerated BAC (termed NBAC) on DOM removal was comprehensively compared in this study. In addition, the effect of pre-ozone and HFM-based aeration on improving BAC performance was compared. Furthermore, to further investigate the feasibility of ABAC for drinking water treatment, water samples after ABAC and conventional coagulation were examined and the DBP formation potentials were evaluated. The results of this study have demonstrated the effectiveness and benefits of the ABAC system, and advanced the potential application of this biofiltration process for drinking water treatment in rural areas.

2. Materials and methods

2.1. Experimental setup and materials

The lab-scale BAC filter was a circular plexiglass column (diameter: 50 mm × height: 450 mm) packed with 480 g granular activated carbon (coconut shell GAC, average particle size of 3 – 5 mm). The packing bed had a height of 400 mm and an effective volume of 300 mL, corresponding to a bed porosity of 0.38. A bubbleless aerated BAC filter, modified from our previous study (Mengjie Liu 2023), was used to provide air throughout the BAC system. As shown in Fig. 1A and 1B, a polyvinylidene difluoride (PVDF) hollow fiber membrane (HFM, diameter: 1.1 mm) module with 14 strips of HFM was installed in a U-shape, and each strip of HFM was separated from others by several pore plates incorporated in the column, as shown in Fig. 1A and 1B. High-pressure air passed through the membrane pores, emerging into the water flow in the form of tiny bubbles (Fig. 1C). The BAC column with HFM modules was termed ABAC (bubbleless aerated BAC filter), and an identical column without HFM modules was termed NBAC (non-aerated BAC filter). Both NBAC and ABAC systems were designed to operate in

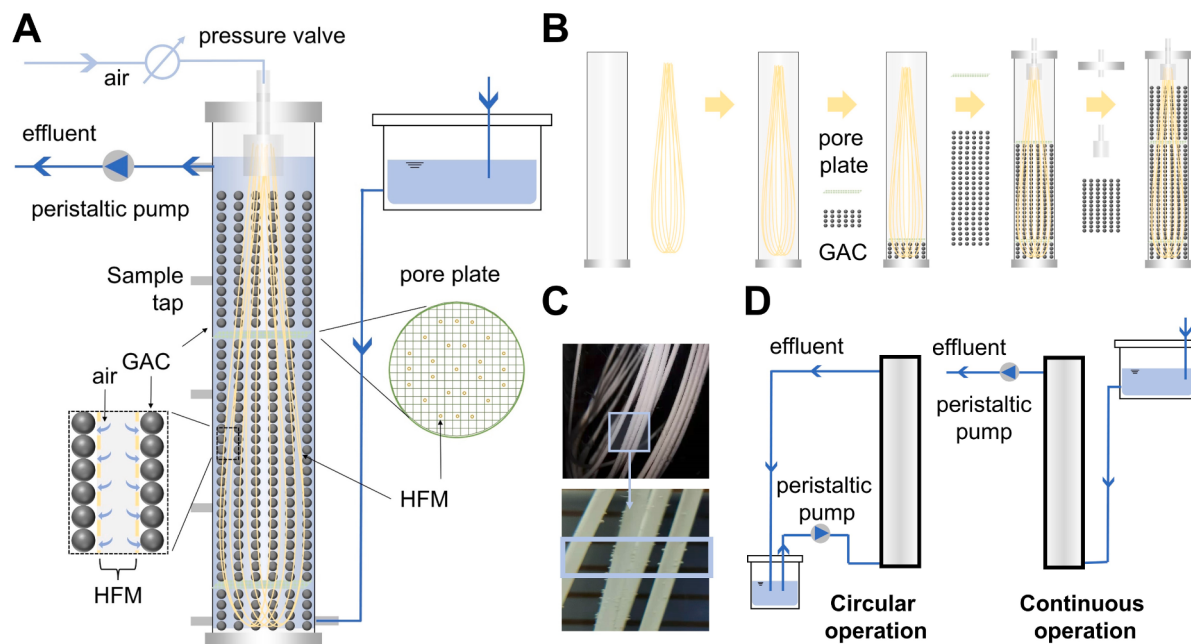


Fig. 1. (A) Schematic of the HFM-aerated gravity flow BAC system; (B) Schematic showing assembly of the ABAC system; (C) Images of air bubbles on HFMs; (D) Two operation modes (circular and continuous) of the BAC systems. In the circular mode, the feed water was pumped to the column using a peristaltic pump with two channels (L100-1S-1-DG-6, Longer pump, China); the water passed upwards from the column bottom and then gravitated back from the top of the column to the feed water tank; in the continuous flow, a tank with a constant water level was used to maintain the water level of the filter column; the feed water passed upwards from the bottom through the column, and a peristaltic pump was used to draw the water at a constant rate. The device was modified from our previous study (Mengjie Liu 2023).

parallel, with the up-flow either in circular (re-cycle) or continuous (single pass) modes, by changing the arrangement of pipe fittings, connections and storage tank (Fig. 1D).

The raw water in this study was sourced from a local natural surface water, the JingMi river (JM), Beijing, China. The JM water is used to provide drinking water for Beijing (SI, Figure S1), and is sourced from the Danjiangkou Reservoir in Hubei province (which belongs to the largest river basin in China: the Yangtze River basin), via the middle route of China's South-North Water Diversion project. The physical and chemical properties of JM water are shown in the supporting information (SI, Table S1). Prior to treating JM water, the BAC filters were inoculated with microorganisms using soil from the Miyun reservoir (SI, Figure S1), and then operated for three weeks to pre-stabilize the performance of the BAC filters. Details about the microbial inoculation and pre-operation of the BAC filters are also described in the SI (Text S1).

2.2. Continuous operation and comparison with other processes

After inoculation and pre-stabilization, the two BAC systems operated continuously at an HRT of 8 h (bed approach velocity, $v_a = 0.02 \text{ m/h}$). During the first 140 days (phase 1), the performance of the two BAC filters, as well as conventional coagulation, for DOM removal was comprehensively compared, and each BAC system had three identical, parallel columns in order to determine its repeatability. The coagulation test was conducted using a flocculator jar test apparatus (MY3000-2 N/4 N, China). Aluminum sulfate ($\text{Al}_2(\text{SO}_4)_3 \bullet 12\text{H}_2\text{O}$), obtained from Sinopharm Chemical Reagent Co. Ltd, was used as the coagulant. Detail information of the coagulation test is provided in the Supporting Information (SI, Text S2).

For the second phase (from day 141 to day 210), the raw water in two of the three parallel columns was replaced by the ozone-pretreated JM water (treated by 3 mg/L or 1.5 mg/L ozone), to compare the effectiveness of pre-ozonation and HFM-based aeration on DOM removal. Ozone was generated from oxygen by an ozone generator (KRC Marine LTD, UK) at an applied pressure of 0.1 MPa and a gas flow rate of 0.1 L/min. The ozone concentration from the generator was measured using a method from a previous study (Di Baldassarre et al. 2018). Different concentrations of ozone (0 – 4 mg/L) were added by controlling the gas-liquid contact time.

2.3. Water quality measurements

The DO concentration at different heights of the filter were measured using a FiveGo DO meter (Mettler Toledo, USA). Water samples were collected from the constant level water tank (R, raw water) and from the outlet of the ABAC (A) and NBAC (N) filters, and were then filtered by a membrane filter (SCAA-201, 25mm×0.22 μm, ANPEL) prior to the following analysis. Dissolved organic carbon (DOC) were measured by a total organic carbon analyzer (TOC-Vvp, Shimadzu, Japan). The molecular weight (MW) distribution was determined by size exclusion chromatography (SEC) equipped with an optical detector (Waters, USA). The SEC peaks were integrated to represent the DOM content of different MW.

The chromophore and fluorescent organic substances were respectively characterized by a UV-visible spectrophotometer (UV-2600, Shimadzu, Japan) and 3D excitation-emission matrix (EEM) spectrofluorometer (F-4600FL, Hitachi, Japan). The elimination of scattering, the correction of the inner filter effect and intensity, and parallel factor (PARAFAC) analysis, were applied to the EEM data using the R software package Stadom (Pucher et al., 2019). In addition, the EEM spectra were divided into five wavelength regions, and their integrals were calculated according to a previous study (Park and Snyder 2018). Several optical parameters were calculated from the EEM and UV-visible spectral data, as shown in the SI, Table S2. A principal component analysis (PCA) was conducted using the R community ecology package, 'vegan' (Oksanen et al., 2022). Function lm from the R package statistics was used to

conduct the linear regression (Team 2022).

Disinfection byproduct (DBP) formation potential (DBPFP) was measured based on the regulated trihalomethane and haloacetic acid compounds. These were determined by a gas chromatograph (Clarus 590, PerkinElmer, U.S.) with an electron capture detector (ECD), following the U.S. Environmental Protection Agency methods 551 and 552.3 (EPA, 1995; 2003). Details of the methods are included in the SI, Texts S3–S4. The measurements of DBPFP were replicated three times for each sample. Specific DBPs was defined as DBP yield per unit DOC (i.e., SDBPs=DBPFP/DOC).

2.4. Characterization of biofilms on activated carbon

At the end of phase 1, the GAC particles from the middle of the six columns (100~300 mm below the water level) were sampled, and rinsed twice with 0.01 M phosphoric acid buffer (PBS, containing 3.2 mM Na_2HPO_4 , 0.5 mM KH_2PO_4 , 1.3 mM KCl and 135 mM NaCl, pH=7.4) for subsequent chemical and microbial characterization. Scanning electron microscopy (SEM, JSM-7001F+INCA X-MAX, Japan) was employed for morphological characterization (SI, Text S5). Extracellular polymeric substances (EPS) were extracted from carbon particles using the heating method as described in Text S6 (SI), and the polysaccharide and protein contents within the EPS were quantified via spectrophotometry methods (DuBois et al., 1956; Bradford 1976). The measurements were replicated three times. Two-gram GAC particles from the six BAC filters were collected for microbial community analysis. After the pre-treatments (SI, Text S7), the samples were subjected to subsequent DNA extraction and 16S rRNA sequencing. Procedures for DNA extraction and 16S rRNA sequencing are described in the SI, Text S7.

3. Results

3.1. Long-term effluent quality

During the 140-day operation (phase 1), the difference in the effluent DOC of the two systems (NBAC and ABAC) gradually increased (Fig. 2A). The DOC removal efficiency of the NBAC process deteriorated substantially after the five-month operation, decreasing from $53 \pm 4\%$ to $38 \pm 2\%$. In comparison, the ABAC process outperformed the NBAC in terms of a sustained stability, exhibiting a consistent removal efficiency >55%, and having a significantly lower effluent DOC value than NBAC (Fig. 2B). Previous studies using sand as filter material for river bank filtration showed a DOC removal of only 5 –15% (Baumgarten et al., 2011; Bertelkamp et al., 2014). By using GAC as a partial or whole filter material, the DOC removal increased from < 20% to > 40% after 12-week operation (Xu et al., 2021a).

According to the results summarized in Fig. 2C, the dissolved oxygen (DO) at the middle (200 mm below the water surface) of ABAC was significantly higher than that of NBAC (ABAC: $4.75 \pm 0.41 \text{ mg/L}$; NBAC: $1.34 \pm 0.21 \text{ mg/L}$). DO has been recognized as an important electron acceptor in biological redox reactions, and therefore can support the growth of heterotrophic bacteria along with the degradation of organic carbon.(Benner et al., 2013) Previous studies have suggested that the progressive depletion of DO within conventional BAC filters led to anoxic conditions and poor degradation efficiency in the middle and downstream regions of the process (Zheng et al., 2010; Chuang and Mitch 2017). The results of this study suggested HFM-based aeration was effective in improving DOC removal.

Fig. 2D demonstrated the difference between the fluorescent DOM in raw water and BAC effluents. Matching the parallel factor (PARAFAC) analysis results with the Openflour database (Murphy et al., 2014) identified three independent fluorescence components (SI, Figure S3): two protein-like (C1 (Dainard et al., 2015; Kida et al., 2019) and C3 (Murphy et al., 2006; Retelletti Brogi et al. 2018)), and one terrestrial humic-like (Henderson et al., 2009; Amaral et al., 2016; Lu et al., 2022) (C2). ABAC showed a significant increase in the removal of both C1 and

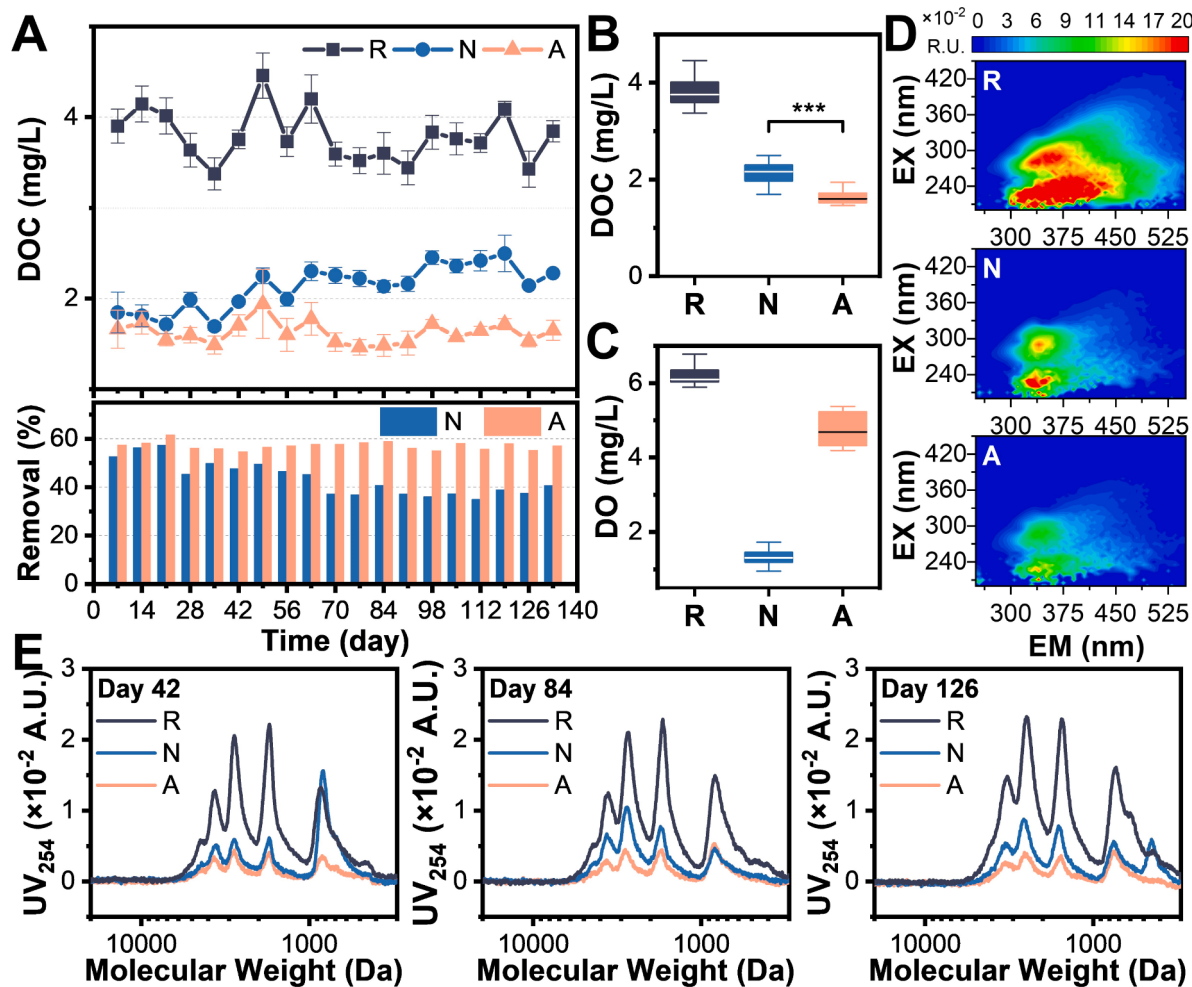


Fig. 2. Water quality of raw water and the effluents from the two BAC processes in the first phase: (A) The variation of DOC value (top) and DOC removal efficiency (bottom) with operation time. Error bars represent the standard deviation; (B – C) Box plot showing the DOC (B) and DO (C) of raw water (R), NBAC effluent (N) and ABAC effluent (A); the box plot displays the five-number summary of a set of data: centerline, median; box limits, upper and lower quartiles; whiskers, $1.5 \times$ interquartile range. Wilcoxon test was conducted between DOC values from the NBAC and ABAC: *** $p < 0.001$; (D) EEM spectra of raw water (R, top), NBAC effluent (N, middle) and ABAC effluent (A, bottom); (E) Apparent molecular weight distribution for raw water (R) and effluents (N and A) at day 42 (left), day 84 (middle) and day 126 (right).

C2 components compared to NBAC (SI, Figure S3), while the difference of C3 was not significant between the two effluents. According to a previous study, biopolymers were more preferably removed than humic substances by biofiltration (Zheng et al., 2010). However, our results demonstrated a > 65% removal of humic-like substances. This might be ascribed to the addition of 20 mg/L of humic acid in the feed water in the pre-stabilization period (SI, Text S1) that favored the enrichment of HA-degrading microorganisms.

From the perspective of molecular weight (MW) distribution, both NBAC and ABAC showed a high degree of removal of high-MW substances ($MW > 1000$ Da) during the first six weeks, but the removal of low-MW fractions ($MW < 1000$ Da) by NBAC was inferior to ABAC (Fig. 2E and SI, Figure S4). After 56 days, the NBAC process exhibited a clear regression in the removal of high-MW substances. In addition, the DOM removal by NBAC was not stable in the long-term operation, as a new peak in the NBAC effluent was observed at day 126, indicating that low-MW organics could not be efficiently degraded. In contrast, the MW distribution pattern of the ABAC effluent showed little variability during the whole operation period, further indicating the high efficiency and strong stability of the ABAC process.

3.2. Variation of dom properties along columns

In order to investigate the change of DOM during the BAC processes, water samples from different heights of the BAC column (i.e., 0 mm, 100 mm, 200 mm, 300 mm and 400 mm, from bottom to top) were collected and subjected to EEM, UV-vis and SEC analysis. According to the DO profile along the bed depth (Fig. 3A), the DO in the NBAC dropped rapidly to 1.43 ± 0.20 mg/L at the height of 100 mm. As the flow moved upward from 300 mm to 400 mm, the DO value gradually increased as a consequence of atmospheric diffusion from the open top of the column. In contrast, the DO concentration in the ABAC system was relatively uniform with height, ensuring an aerobic environment throughout the system.

Fig. 3B showed the MW distribution of the DOM at different heights, and Fig. 3C quantified the integrated area of the four principal MW peaks. It was noticed that P4 (MW: 300 – 1000 Da) increased at a bed height of 100 mm for both BAC systems, which was attributed to the degradation of high-MW substances to low-MW substances. As the bed height increased, the low-MW substances gradually mineralized and thus P4 decreased. Another interesting finding was that at the anaerobic zone of the NBAC system (i.e., height 100 – 300 mm), the degradation of high-MW ($MW > 1000$ Da) was much less than ABAC. Specifically, from height = 100 mm to height = 300 mm, P1, P2 and P3 decreased by 38%,

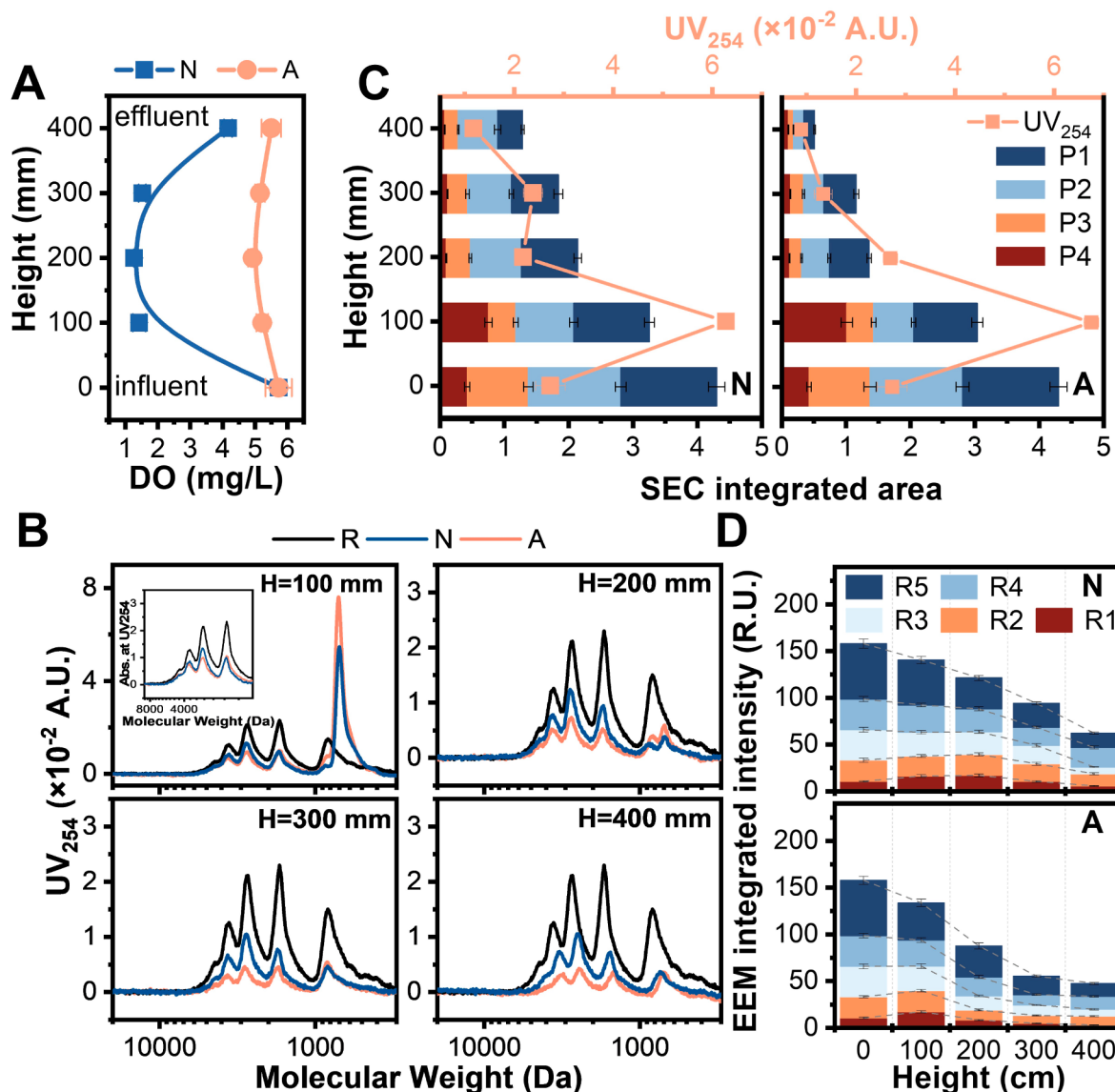


Fig. 3. Water quality of the raw water and the effluents from the two BAC systems at different heights (0 mm, 100 mm, 200 mm, 300 mm and 400 mm, samples at 0 mm and 400 mm were collected at the constant level tank and the effluent tank, respectively): (A) DO concentration – filter height profiles for the NBAC and ABAC systems. Error bars represent the standard deviation; (B) Apparent molecular weight distribution for raw water (R) and BAC effluents (N and A); (C) Absorbance at 254 nm (line plot) and integrated area of the four SEC peaks (bar plot): P1 (3000 – 10,000 Da), P2 (2000 – 3000 Da), P3 (1000 – 2000 Da), P4 (300 – 1000 Da). N is for NBAC (left) and A is for ABAC (right). Error bars represent the standard deviation; (D) EEM regional integrated fluorescence intensity. Error bars represent the standard deviation. R1: tyrosine-like aromatic protein; R2: tryptophan-like aromatic protein; R3: fulvic acid-like matter; R4: soluble microbial byproduct-like matter; R5: humic acid-like matter. N is for NBAC (top) and A is for ABAC (bottom).

24% and 26% respectively for NBAC, while P1, P2 and P3 decreased by 49%, 49% and 51% respectively for ABAC. These results suggested that maintaining aerobic conditions favored the degradation of high-MW substances. UV-vis and EEM spectra also confirmed the benefit of high DO on the removal of chromophore and fluorescent organic substances (Figs. 3C, 3D and S5 (SI)). In addition, according to these results, the DOM content at the height of 300 mm for the ABAC process (A300 sample) was lower than the DOM content at the height of 400 mm for the NBAC process (N400 sample), indicating that shortening the HRT of the ABAC system to 6 h could still achieve a better DOM removal performance than the NBAC with a HRT of 8 h.

3.3. Characterization of bac particles

After the 140-day operation (phase 1), BAC particles from the NBAC and ABAC filters were taken out and characterized. The SEM results

revealed apparent morphological differences between the carbon particles from the NBAC and ABAC filters (Figs. 4A, S6 and S7 (SI)). Carbon particles from NBAC were completely covered by biofilms, with the bacteria being encased in a thick extracellular polymer substance (EPS). In contrast, individual bacteria can be easily distinguished on carbon particles from the ABAC system, and most of the activated carbon surface was exposed in water, making it conducive to adsorb organic matter for subsequent microbial degradation. Moreover, EPS has been reported to hinder extracellular electron transfer in biofilms (Wang et al., 2021a), and therefore the large amount of secreted protein and polysaccharide (Fig. 4B) decreased the degradation of DOM by biological activities.

In addition to the structure of biofilm, the differences in the microbial community composition were also responsible for the differences in DOM removal. Unconstrained principal coordinate analyses (PCoAs) of the Bray-curtis distance were performed to demonstrate the differences of microbial communities between ABAC, and NBAC. The Bray-curtis

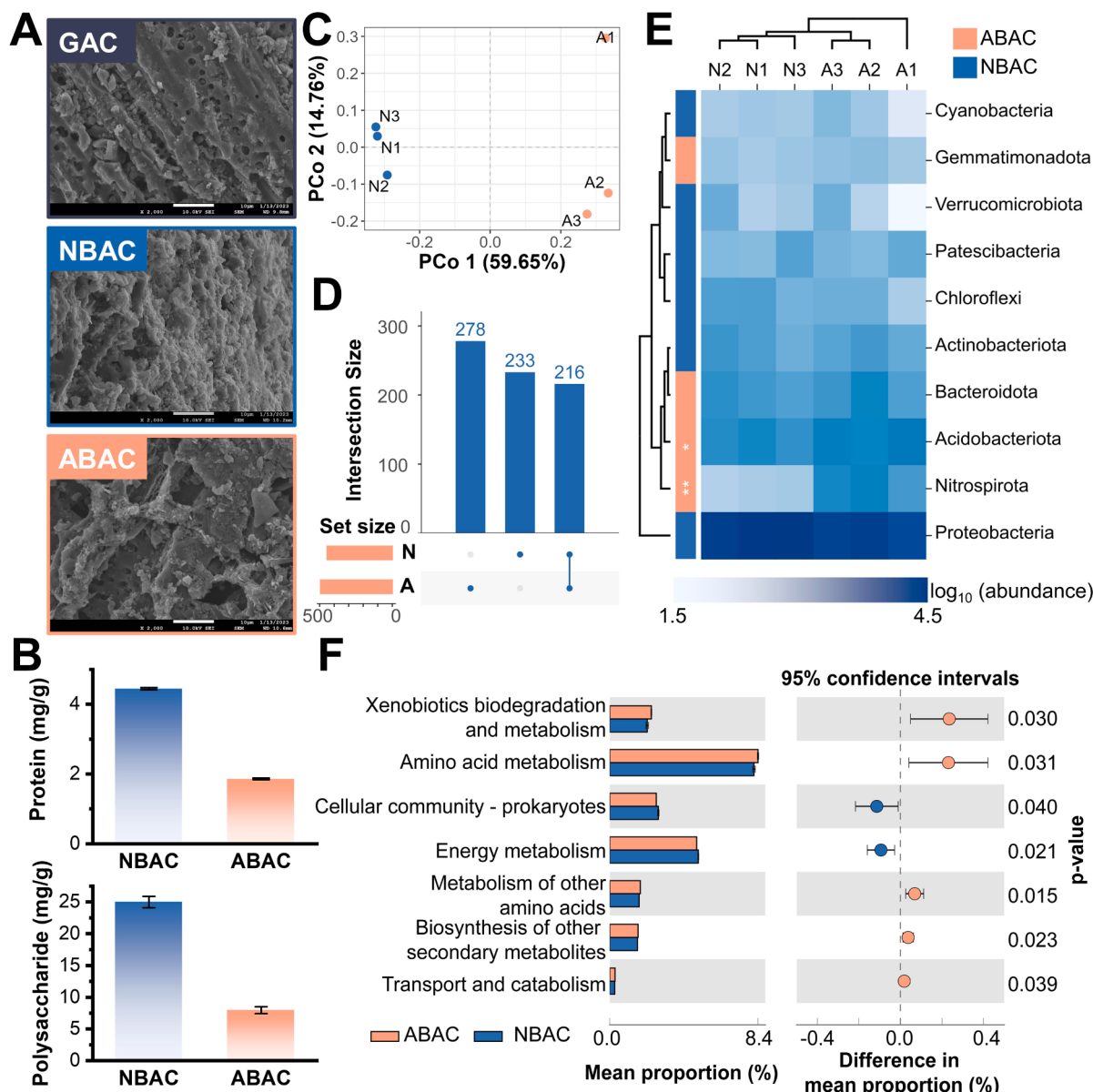


Fig. 4. Characterization of BAC particles: (A) Surface morphology of GAC (top), NBAC (middle) and ABAC (bottom) particles; (B) Protein (top) and polysaccharide (bottom) content of EPS from NABC and ABAC particles. Error bars represent the standard deviation; (C) Overall principal coordinate analysis (PCoA) of bacterial communities in the ABAC (A1–A3, orange) and NBAC (N1–N3, blue); (D) UpSetView showing the OTU numbers in the ABAC and NBAC systems. OTU with relative abundance > 10% were counted; (E) Heatmap illustrating the relative abundances of bacterial communities at the phylum level (top 10) based on 16S rRNA sequencing. N1–N3 are three NBAC samples, and A1–A3 are three ABAC samples. The bar color at left side (blue and orange) indicated groups with higher abundance (NBAC or ABAC), and the significance was evaluated by Wilcoxon test: *, $0.01 \leq p < 0.05$; **, $0.001 \leq p < 0.01$. The cluster analysis was conducted based on braycurtis distance; (F) Extended bar plot showing the function prediction results by PICRUSt2 at KEGG level 2. ABAC and NABC groups were compared by Welch's t-test, and the p-value was labeled at the right side. Categories with p-value greater than 0.05 were not shown. (For interpretation of the references to colour in this figure legend, the reader is referred to the web version of this article.)

distance was calculated from the normalized OTU tables using the R package Vegan (Oksanen et al., 2022). It was suggested that ABAC and NBAC had significant differences in microbial composition (Fig. 4C). ABAC and NBAC samples were separated along the first PCoA axis that accounted for 59.65% of the total variance. Fig. 4D suggested that ABAC and NBAC shared 216 OTUs, and their exclusive OTUs accounted for 56% and 52% of the total OTUs, respectively.

At the phylum level, *proteobacteria* was the most abundant phylum in both BAC systems, accounting for 65% and 53% of the relative abundance in the NBAC and ABAC filters, respectively. ABAC showed a significantly high abundance of *Nitrospirota* and *Acidobacteriota* (Fig. 4E). *Nitrospirota* is an aerobic bacterium that reduces ammonia,

nitrogen and nitrite concentrations (Lautenschlager et al., 2014), implying that enhanced DO in ABAC filters can also favor nitrification processes in BAC filters. Acidobacteriota are highly abundant in soils (Gonçalves and Santana 2021); most members of this phylum are aerobes that prefer sugars as a source of carbon and energy, and are capable of degrading complex carbohydrates (Kuramae and de Assis Costa 2019). LEfSe results (LDA>3) further revealed the differences between the two systems at the class level (SI, Figure S8). For instance, *Alphaproteobacteria* and *Gamaproteobacteria* are two subcategories in the *Proteobacteria* phylum. The former are significantly enriched in ABAC, have been reported to be competitive at low nutrient concentrations, and can degrade complex organic compounds such as humic acid (Newton et al.,

2011; Lu et al., 2020). On the contrary, NBAC had more *Gamaproteobacteria*, the members of which have been reported to exhibit a fast growth rate, especially in the presence of nitrogen and phosphorus (Šimek et al., 2006).

PICRUSt2 analysis provided more information regarding the function of the two microbial communities. The metabolic pathways account for more than 75% of the identified pathways at KEGG level 1 for both systems. For KEGG level 2, ABAC showed a significantly higher proportion in the metabolism of Xenobiotics and amino acid than NBAC (Fig. 4F), which were in good agreement with the characterization described above and explain the higher removal efficiency in the ABAC system.

3.4. Comparison of bubbleless aeration and pre-ozonation

Ozonation has been proposed as an effective pretreatment for the BAC process in many research studies and applications (Lin et al., 2001; Sundaram et al., 2020). Previous studies have suggested that pre-ozonation can improve the biodegradability of organic matter, and thus enhance the DOM removal efficiency by subsequent BAC (Lin et al., 2001). Figs. 5A and S9 (SI) showed DOC residue (%) by different concentrations of ozone and the DBPFP of treated samples. Ozone had a poor mineralization effect on natural organic matter, with the DOC

removal of 17% at the highest concentration of 4 mg/L (SI, Figure S9A). An apparent reduction of high-MW substances was observed, but organic matter with MW < 1000 showed little change as the ozone concentration increased from 1 to 4 mg/L (SI, Figure S9B). With respect to the DBPFP, when the ozone < 2.5 mg/L (SI, Figure S9C), the THMFP increased with ozone concentration, which is consistent with previous studies showing a low concentration of ozone increased THM formation (Liu et al., 2022b). In consideration of the above results, two concentrations were chosen (i.e., 1.5 mg/L and 3 mg/L) for the subsequent comparison of pre-ozonation and bubbleless aeration.

After ozonation, the DO concentration of the raw water increased, but only a high concentration of ozone treatment (3 mg/L) led to a significant increase of DO for both NBAC and ABAC systems (Fig. 5B). The DOC of the NBAC effluent showed 5% and 11% reductions by 1.5 mg/L and 3 mg/L pre-ozonation, respectively. In comparison, the ABAC without pre-ozonation reached 20% reduction of DOC, and pre-ozonation showed an insignificant further increase in DOC removal. Therefore, the results indicate that bubbleless aeration, by increasing the DO within the BAC system, enhanced its performance more effectively than pre-ozonation. Despite the high reactivity of ozone with unsaturated bonds and aromatic structures (Von Sonntag and Von Gunten 2012; Phungsai et al., 2019), the contents of chromophore and fluorescent organic substances in the ABAC effluent were still lower than

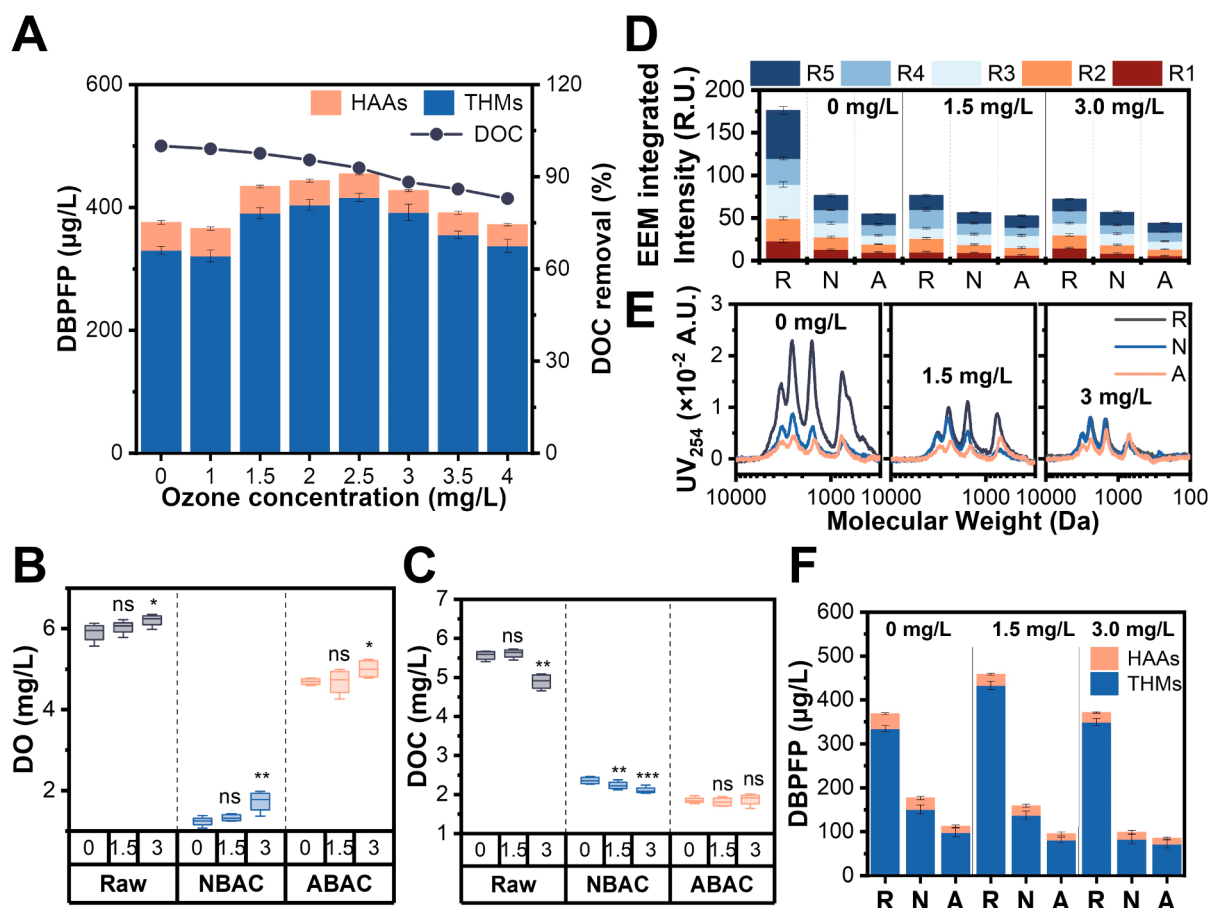


Fig. 5. Comparison of bubbleless aeration and pre-ozonation. R, N, A represent raw water, NBAC effluent and ABAC effluent; the numbers 0, 1.5 and 3 represent ozone concentration. (A) DBP formation potential (DBPFP, bar plot) and DOC removal efficiency (line plot) for raw water treated by different concentrations of ozone. Error bars represent the standard deviation; (B – C) Box plots showing the DO (B) and DOC (C) of raw water, NBAC effluent and ABAC effluent. The box plot displays the five-number summary of a set of data: centerline, median; box limits, upper and lower quartiles; whiskers, $1.5 \times$ interquartile range; points, maximum and minimum values. Wilcoxon test was conducted between pre-ozone samples (1.5 mg/L and 3 mg/L) and non-ozone samples (0 mg/L): ns, $p \geq 0.05$; *, $0.01 \leq p < 0.05$; **, $0.001 \leq p < 0.01$; ***, $p < 0.001$; (D) EEM regional integrated fluorescence intensity. Error bars represent the standard deviation. R1: tyrosine-like aromatic protein; R2: tryptophan-like aromatic protein; R3: fulvic acid-like matter; R4: soluble microbial byproduct-like matter; R5: humic acid-like matter; (E) Apparent molecular weight distribution; (F) DBP formation potential for raw water pretreated by different concentrations of ozone (R), NBAC (N) and ABAC (A). Error bars represent the standard deviation.

the ozone-NBAC (Figs. 5D, 5E and S10 (SI)). Compared to NBAC alone, the DBPFP decreased by 36%, 10% and 44% with bubbleless aeration, 1.5 mg/L pre-ozonation and 3 mg/L pre-ozonation, respectively (Figs. 5F and S11 (SI)). However, the application of 3 mg/L ozone is likely to be expensive for drinking water treatment, and the operation and maintenance of ozone generation equipment more sophisticated and demanding than the bubbleless aeration. Therefore, ABAC is likely to be more suitable for rural drinking water treatment than an ozone-BAC process.

3.5. Comparison with coagulation

Coagulation is one of the most common drinking water treatment processes. According to the results of a principal component analysis (PCA), shown in Fig. 6A, the difference between raw water samples, coagulated samples and BAC effluents accounted for 63.23% of the total variance. The NBAC and ABAC samples are separated along the second principal axis with an explained variance of 20.11%. In addition, water samples after lab-scale coagulation showed similar water qualities to tap water from the municipal water supply, in terms of the DOC, EEM components and MW distributions (SI, Figures S12 and S13). Therefore,

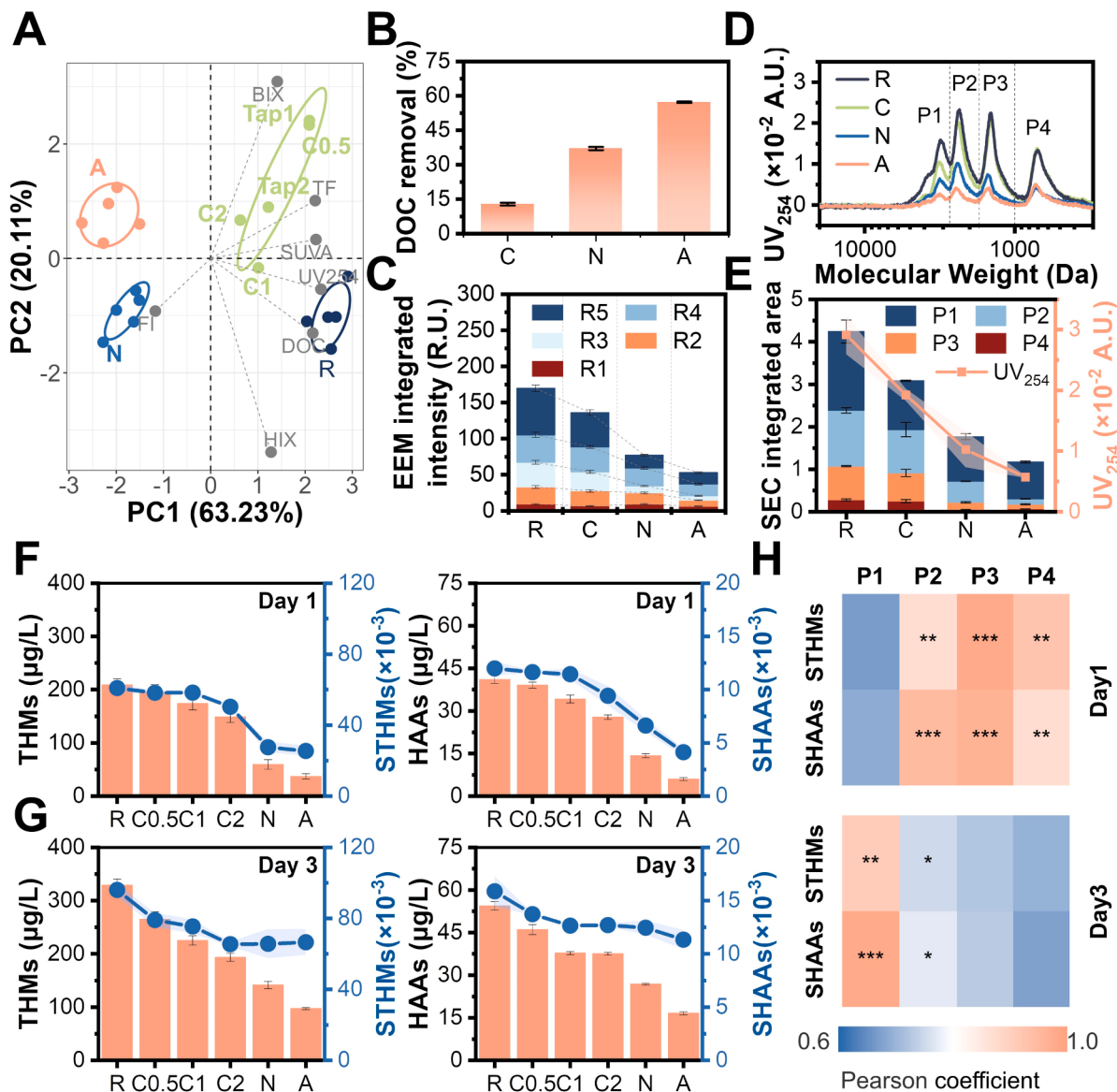


Fig. 6. Comparison with coagulation. R, N, A represent raw water, NBAC effluent and ABAC effluent; C represents coagulated water, with the suffixes 0.5, 1 and 2 indicating the concentration of coagulant: C0.5, 0.05 mM Al³⁺; C1, 0.1 mM Al³⁺; C2, 0.2 mM Al³⁺. (A) PCA results showing the difference among raw water (dark blue), NBAC effluent (blue), ABAC effluent (orange) and coagulated samples (lab-scale coagulation and municipal tap water, green). The gray points are water indexes: DOC, ultraviolet absorbance at 254 nm (UV₂₅₄), specific ultraviolet absorbance at 254 nm (SUVA), fluorescence index (FI), biological index (BIX), humification index (HIX), and TF (total fluorescence); (B) DOC removal efficiency of coagulation (C), NBAC (N) and ABAC (A). Error bars represent the standard deviation; (C) EEM regional integrated fluorescence intensity. Error bars represent the standard deviation. R1: tyrosine-like aromatic protein; R2: tryptophan-like aromatic protein; R3: fulvic acid-like matter; R4: soluble microbial byproduct-like matter; R5: humic acid-like matter; (D) Apparent molecular weight distribution; (E) Absorbance at 254 nm (line plot) and integrated area of the four SEC peaks (bar plot): P1 (3000 – 10,000 Da), P2 (2000 – 3000 Da), P3 (1000 – 2000 Da), P4 (300 – 1000 Da). Error bars represent the standard deviation; (F – G) THM or HAA formation potential (bar plot) and STHMs or SHAAs (specific DBPs = DBPs/DOC, line plot) after 1-day (F) and 3-day (G) incubation. Error bars represent the standard deviation; (H) Heatmap showing the Pearson correlation between SDBPs and integrated area of the four SEC peaks, the asterisks denote the significance levels: ***p < 0.001, **p < 0.01 and *p < 0.05. (For interpretation of the references to colour in this figure legend, the reader is referred to the web version of this article.)

water sample coagulated with 0.1 mM Al³⁺ was used as a comparison to test the performance of BAC in drinking water treatment.

The DOC removal efficiency of coagulation, NBAC and ABAC processes were $13 \pm 0.6\%$, $37 \pm 0.7\%$ and $57 \pm 0.3\%$, respectively (Fig. 6B). It is known that hydrolyzing metal-based coagulation removes organic matter mainly by charge neutralization and sweep flocculation, and organics with higher MW are easier to be removed. For instance, a previous study using high-resolution mass spectra found that the molecular weight distribution of the coagulated water sample substantially skewed towards lower MW compared to raw water, indicating that coagulation preferentially removed substances with higher MW (Liu et al., 2022b). Coagulation showed a poor removal efficiency (< 20%) of fluorescent substances, while NBAC and ABAC degraded 55% and 69% fluorescent substances, respectively (Fig. 6C). Organic substance with MW >3000 was preferentially removed by coagulation, with a 38% removal efficiency (Figs. 6D and 6E). In comparison, coagulation showed little removal of components with MW < 3000 Da, where the removal was only 19%, compared with 70% for NBAC and 87% for ABAC.

The control of disinfection byproducts (DBPs) in drinking water has attracted great attention in recent decades (Liu et al., 2022a; Lau et al., 2023). Here, DBP formation potential (DBPFP) was measured by adding a specific amount of chlorine (3 times the DOC value) to the treated water samples and incubating them in the dark for 1 day or 3 days (Du et al., 2022). It was found that after 1-day incubation, the DBP concentrations in coagulated samples were close to the DBP concentrations in real tap water (SI, Figure S14), where the differences might be attributed to the additional treatment of the tap water (e.g., filtration), difference in disinfection reagents, concentration and time. For the 1-day incubation, the DBPFP for coagulation, NBAC and ABAC were $176.7 \pm 6.7 \mu\text{g/L}$, $73.7 \pm 7.7 \mu\text{g/L}$ and $43.4 \pm 4.8 \mu\text{g/L}$, respectively; these represent a decrease of $30 \pm 3\%$, $71 \pm 3\%$ and $83 \pm 2\%$ compared to raw water, respectively. For the 3-day incubation, the reductions were $31 \pm 3\%$, $56 \pm 5\%$ and $70 \pm 3\%$ for coagulation, NBAC and ABAC, respectively (Figs. 6F and 6G).

Variations of the DBPFP with incubation time indicate dynamic changes of disinfection byproduct formation. Specific DBPs are defined as the DBPs formed per unit of DOC, and the corresponding results are shown in Figs. 6F and 6G. For the 1-day incubation, the SDBPs formation for coagulated water was comparable to the raw water, but were substantially lower than coagulated water for the BAC effluents. However, for the 3-day incubation, the differences in SDBPs between coagulated water and the BAC effluents were much less. Among the five EEM components, R3 (fulvic acid-like matter) and R5 (humic acid-like matter) were the major components (i.e., accounting for the major portion of the DOM), and hence their intensity was significantly correlated with the SDBPs for 1-day of incubation (SI, Figure S12). However, after 3 days of incubation, SHAAs were significantly correlated with all EEM components, suggesting that fluorescent organic matter is an important precursor of HAAs. Previous studies have also suggested that while aliphatic structures resulted in THM formation, HAAs had more aromatic structures as their precursors (Liang and Singer 2003; Hua and Reckhow 2007; Zhang et al., 2012).

The relationships between the SDBPs and the MW of DOM were further examined and demonstrated in Figs. 6H, S15 and S16 (SI). For the 1-day incubation time, both STHMs and SHAAs showed significant correlation with low-MW components (MW < 3000 Da), while for the 3-day incubation, the SDBPs were significantly correlated with high-MW components (MW > 3000 Da). These results implied that organic matter reacts with chlorine to produce THMs and HAAs in the order of low to high MW range, with more time required for high MW organic matter to be attacked by chlorine to produce the selected DBPs (i.e., THMs and HAAs). For short incubation times (e.g. flow transport in municipal pipelines), the chlorinated intermediates generated from high-MW organic fractions might be more harmful (toxicologically significant) than the regulated DBPs (Jiang et al., 2020; Han et al., 2021). Therefore,

when discussing the removal of DBP precursors by drinking water treatment processes, the experimental results may not necessarily reflect the actual situation in practice. Removing as much of the pool of organic substances as possible is a ‘first-principles’ approach to reducing DBP formation during the water treatment process. In addition to this, for a small-scale/decentralized drinking water treatment scheme, with a short pipeline transport time, the results here suggested BAC effluents would have SDBPs of less than half of coagulated water SDBPs.

4. Discussion

The first target under the UN Sustainable Development Goal (SDG) 6, Target 6.1, is, “By 2030, achieve universal and equitable access to safe and affordable drinking water for all”. It was reported that a total of 466.7 billion yuan has been invested in rural water supply projects in China, providing safe drinking water to 280 million rural residents, and 84% of rural areas have access to tap water in the last decade. Nonetheless, achieving the SDG target 6.1 remains a long way off, and rural drinking water supply still faces many challenges due to economic, topographical, water resources and labor constraints. Small municipalities are often too far removed from political and industrial interests to afford complex multi-stepped treatment systems (Scheili et al., 2015). Therefore, decentralized and small-scale water systems are an important component of rural water supply. In the past, most rural villages used self-sustaining water sources, such as wells/cellars or small pond sources, and used raw water directly without treatment. Substandard water supply and water quality are practical issues that need to be urgently addressed in the development of rural water supply projects.

Slow sand filtration and riverbank filtration have the advantages of low operating cost and simple operation, making them suitable for rural drinking water projects (Hu et al., 2016). However, the flow residence time is relatively long (typically several to dozens of hours), and the purifying efficiency is very low (DOC removal < 30%) (Rudolf von Rohr et al. 2014; Ahmed and Marhaba 2017; Freitas et al., 2022). Granular activated carbon (GAC), with its beneficial properties of high specific surface area, well-developed pore structure and excellent adsorption performance, is also conducive to microbial attachment, so as to form biofilms to degrade pollutants. Enhancement of the latter effect has led to the development of the biological activated carbon (BAC) process, which was first used for the treatment of municipal or industrial wastewater (Lin et al., 2001; Sauter et al., 2023). In recent years, the ozone-BAC process has been widely applied to enhance drinking water treatment to improve the water quality and decrease the precursors of disinfection byproducts (DBPs) (Wan et al., 2021; Hou et al., 2022). Some studies have also proposed the combination of ozone-BAC with membrane filtration for wastewater reuse (Lau et al., 2023). However, the deficiency of dissolved oxygen within the BAC bed limits the biological degradation in BAC processes, especially for slow rate BAC processes. In trying to ameliorate this, the use of large-scale aeration facilities or pre-ozonation treatment is likely to significantly increase the operational and maintenance costs, and reduce the sustainability and appropriateness of the treatment technology for rural drinking water projects. In this study, by incorporating a uniform array of hollow fiber membrane (HFM) filaments in a BAC bed, sufficient oxygen via pressurized air was provided throughout the whole BAC system. Thus, the DOC removal rate was substantially increased from $37 \pm 0.7\%$ and $57 \pm 0.3\%$. The elevated DO value in the ABAC filter enhanced the biodegradation of DOM in two respects: firstly, the biofilm secreted less EPS, which has been reported to hinder extracellular electron transfer (Wang et al. 2021); secondly, the microbial community was shaped by the high level of DO concentration in the ABAC, and exhibited a significantly stronger microbial degradation ability. From a practical point of view, the BAC process outperformed the conventional coagulation process in terms of both DOM removal and DBP (THMs and HAAs) control. Besides, HFM based aeration showed a greater enhancement of the BAC process compared to pre-ozonation. Instead of oxygen that is used for ozone

production, air was used in HFM-based aeration. Moreover, the bubbleless aeration has the advantage of uniform mass transfer and low maintenance (Aybar et al., 2014; Hou et al., 2019; Zhang et al., 2022), greatly saving the quantity of air required for aeration and the operation cost.

In addition to its high treatment efficiency, as demonstrated, the ABAC process can be combined with microfiltration or ultrafiltration, and integrated into an all-in-one device to serve water supply areas of varying flow capacities. The large size of the GAC particles (3–5 mm) ensures safe and reliable operation without backwash (Xu et al., 2021b), and the process is free of chemical addition and discharge. Our previous studies have shown that the ABAC can operate stably for more than 400 days without backwashing, while the removal efficiency of NBAC gradually deteriorated with the operation time (Liu et al., 2023). Such compact, prefabricated drinking water treatment equipment is well-suited to small-scale water systems, and avoids the need for frequent management (low labor and maintenance costs). Therefore, the proposed ABAC process is recommended as a superior drinking water treatment for rural areas.

5. Conclusion

Bubbleless in-bed aeration provides uniform oxygen throughout the whole BAC system, and thus enhances DOM removal. Compared to a conventional BAC system, the DOC removal efficiency increased by 54%, and the DBPFP decreased by 41%. The high DO (> 4 mg/L) in the ABAC process promoted the biodegradation of exogenous organic matter by decreasing the EPS secretion and modifying the microbial community. Bubbleless aeration is more effective and practical, and less costly, for improving BAC performance than applying pre-ozonation, especially for rural drinking water projects. Compared to conventional coagulation, ABAC is a competitive process for small-scale or decentralized drinking water treatment systems, due to its high efficiency and low maintenance.

Declaration of Competing Interest

The authors declare that they have no known competing financial interests or personal relationships that could have appeared to influence the work reported in this paper.

Data availability

Data will be made available on request.

Associated content

All data needed to evaluate the conclusions in the paper are presented in the paper and/or the Supplementary Materials. Additional data relating to this paper may be requested from the authors.

Notes

The authors declare no competing interests.

Acknowledgments

This work was financially supported by the Natural Science Foundation of China (No. 8192042), and the Key Research and Development Plan of the Chinese Ministry of Science and Technology (No. 2019YFC1906501).

Supplementary materials

Supplementary material associated with this article can be found, in

the online version, at doi:10.1016/j.watres.2023.120089.

References

- Ahmed, A.K.A., Marhaba, T.F., 2017. Review on river bank filtration as an in situ water treatment process. *Clean Technol. Environ. Pol.* 19, 349–359.
- Amaral, V., D. Graeber, D. Calliari, and C. Alonso. 2016. Strong linkages between DOM optical properties and main clades of aquatic bacteria. 61:906–918.
- Aybar, M., Pizarro, G., Boltz, J.P., Downing, L., Nerenberg, R., 2014. Energy-efficient wastewater treatment via the air-based, hybrid membrane biofilm reactor (hybrid MfBR). *Water Sci. Technol.* 69, 1735–1741.
- Bauer, R., Dizer, H., Graeber, I., Rosenwinkel, K.-H., López-Pila, J.M., 2011. Removal of bacterial fecal indicators, coliphages and enteric adenoviruses from waters with high fecal pollution by slow sand filtration. *Water Res.* 45, 439–452.
- Baumgarten, B., Jährig, J., Reemtsma, T., Jekel, M., 2011. Long term laboratory column experiments to simulate bank filtration: factors controlling removal of sulfamethoxazole. *Water Res.* 45, 211–220.
- Bei, E., Wu, X., Qiu, Y., Chen, C., Zhang, X., 2019. A tale of two water supplies in china: finding practical solutions to urban and rural water supply problems. *Acc. Chem. Res.* 52, 867–875.
- Benner, J., Helbling, D.E., Kohler, H.-P.E., Wittebol, J., Kaiser, E., Prasse, C., Ternes, T.A., Albers, C.N., Aamand, J., Horemans, B., Springael, D., Walravens, E., Boon, N., 2013. Is biological treatment a viable alternative for micropollutant removal in drinking water treatment processes? *Water Res.* 47, 5955–5976.
- Bertelkamp, C., Reungoat, J., Cornelissen, E.R., Singhal, N., Reynisson, J., Cabo, A.J., van der Hoek, J.P., Verlieerde, A.R.D., 2014. Sorption and biodegradation of organic micropollutants during river bank filtration: a laboratory column study. *Water Res.* 52, 231–241.
- Bradford, M.M., 1976. A rapid and sensitive method for the quantitation of microgram quantities of protein utilizing the principle of protein-dye binding. *Anal. Biochem.* 72, 248–254.
- Chang, H., Yu, H., Li, X., Zhou, Z., Liang, H., Song, W., Ji, H., Liang, Y., Vidic, R.D., 2022. Role of biological granular activated carbon in contaminant removal and ultrafiltration membrane performance in a full-scale system. *J. Memb. Sci.* 644, 120122.
- Chuang, Y.-H., Mitch, W.A., 2017. Effect of Ozonation and Biological Activated Carbon Treatment of Wastewater Effluents on Formation of N-nitrosamines and Halogenated Disinfection Byproducts. *Environ. Sci. Technol.* 51, 2329–2338.
- Dainard, P.G., Guégan, C., McDonald, N., Williams, W.J., 2015. Photobleaching of fluorescent dissolved organic matter in beaufort sea and North Atlantic subtropical gyre. *Mar Chem* 177, 630–637.
- Di Baldassarre, G., Wanders, N., AghaKouchak, A., Kuil, L., Rangecroft, S., Veldkamp, T.I. E., Garcia, M., van Oel, P.R., Breinl, K., Van Loon, A.F., 2018. Water shortages worsened by reservoir effects. *Nature Sustainability* 1, 617–622.
- Du, L., Liu, Y., Hao, Z., Chen, M., Li, L., Ren, D., Wang, J., 2022. Fertilization regime shifts the molecular diversity and chlorine reactivity of soil dissolved organic matter from tropical croplands. *Water Res.* 225, 119106.
- DuBois, M., Gilles, K.A., Hamilton, J.K., Rebers, P.A., Smith, F., 1956. Colorimetric Method for Determination of Sugars and Related Substances. *Anal. Chem.* 28, 350–356.
- EPA, U. S., 1995. Method 551.1: Determination of Chlorination Disinfection Byproducts, Chlorinated Solvents, and Halogenated Pesticides/Herbicides in Drinking Water By Liquid-Liquid Extraction and Gas Chromatography With Electron-Capture Detection. Revision 1.0. Cincinnati, OH.
- EPA, U.S. 2003. Method 552.3: determination of haloacetic acids and dalapon in drinking water by liquid-liquid microextraction, derivatization, and Gas chromatography with electron capture detection. EPA 815-B-03-002. Revision 1.0.
- Freitas, B.L.S., Terin, U.C., Fava, N.M.N., Maciel, P.M.F., Garcia, L.A.T., Medeiros, R.C., Oliveira, M., Fernandez-Ibanez, P., Byrne, J.A., Sabogal-Paz, L.P., 2022. A critical overview of household slow sand filters for water treatment. *Water Res.* 208, 117870.
- Gillefalk, M., G. Massmann, G. Nützmann, and S. Hilt. 2018. Potential impacts of induced bank filtration on surface water quality: a conceptual framework for future research. 10:1240.
- Gonçalves, O.S., Santana, M.F., 2021. The coexistence of monopartite integrative and conjugative elements in the genomes of Acidobacteria. *Gene* 777, 145476.
- Hallé, C., Huck, P.M., Peldszus, S., Haberkamp, J., Jekel, M., 2009. Assessing the performance of biological filtration as pretreatment to low pressure membranes for drinking water. *Environ. Sci. Technol.* 43, 3878–3884.
- Han, J., Zhang, X., Jiang, J., Li, W., 2021. How much of the total organic halogen and developmental toxicity of chlorinated drinking water might be attributed to aromatic halogenated DBPs? *Environ. Sci. Technol.* 55, 5906–5916.
- Henderson, R.K., Baker, A., Murphy, K.R., Hamblly, A., Stuetz, R.M., Khan, S.J., 2009. Fluorescence as a potential monitoring tool for recycled water systems: a review. *Water Res.* 43, 863–881.
- Hou, C., Chen, L., Dong, Y., Yang, Y., Zhang, X., 2022. Unraveling dissolved organic matter in drinking water through integrated ozonation/ceramic membrane and biological activated carbon process using FT-ICR MS. *Water Res.* 222, 118881.
- Hou, D., Jassby, D., Nerenberg, R., Ren, Z.J., 2019. Hydrophobic gas transfer membranes for wastewater treatment and resource recovery. *Environ. Sci. Technol.* 53, 11618–11635.
- Hu, B., Teng, Y., Zhai, Y., Zuo, R., Li, J., Chen, H., 2016. Riverbank filtration in China: a review and perspective. *J. Hydrol. (Amst)* 541, 914–927.
- Hua, G., Reckhow, D.A., 2007. Characterization of Disinfection Byproduct Precursors Based on Hydrophobicity and Molecular Size. *Environ. Sci. Technol.* 41, 3309–3315.

- Jantarakasem, C., Kasuga, I., Kurisu, F., Furumai, H., 2020. Temperature-dependent ammonium removal capacity of biological activated carbon used in a full-scale drinking water treatment plant. *Environ. Sci. Technol.* 54, 13257–13263.
- Jiang, J., Han, J., Zhang, X., 2020. Nonhalogenated aromatic dbps in drinking water chlorination: a gap between nom and halogenated aromatic DBPs. *Environ. Sci. Technol.* 54, 1646–1656.
- Kida, M., Kojima, T., Tanabe, Y., Hayashi, K., Kudoh, S., Maie, N., Fujitake, N., 2019. Origin, distributions, and environmental significance of ubiquitous humic-like fluorophores in Antarctic lakes and streams. *Water Res.* 163, 114901.
- Pages 1-8 in Kuramae, E.E., de Assis Costa, O.Y., 2019. Acidobacteria, editor. In: Schmidt, T.M. (Ed.), Encyclopedia of Microbiology (Fourth Edition). Academic Press, Oxford.
- Lau, S.S., Bokenkamp, K., Tecza, A., Wagner, E.D., Plewa, M.J., Mitch, W.A., 2023. Toxicological assessment of potable reuse and conventional drinking waters. *Nature Sustainability* 6, 39–46.
- Lautenschlager, K., Hwang, C., Ling, F., Liu, W.-T., Boon, N., Köster, O., Egli, T., Hammes, F., 2014. Abundance and composition of indigenous bacterial communities in a multi-step biofiltration-based drinking water treatment plant. *Water Res.* 62, 40–52.
- Liang, L., Singer, P.C., 2003. Factors influencing the formation and relative distribution of haloacetic acids and trihalomethanes in drinking water. *Environ. Sci. Technol.* 37, 2920–2928.
- Lin, C.-K., Tsai, T.-Y., Liu, J.-C., Chen, M.-C., 2001. Enhanced biodegradation of petrochemical wastewater using ozonation and bac advanced treatment system. *Water Res.* 35, 699–704.
- Liu, M., Graham, N., Wang, W., Zhao, R., Lu, Y., Elimelech, M., Yu, W., 2022a. Spatial assessment of tap-water safety in China. *Nature Sustainability* 5, 689–698.
- Liu, M., Graham, N.J.D., Xu, L., Zhang, K., Yu, W., 2023. Bubbleless air shapes biofilms and facilitates natural organic matter transformation in biological activated carbon. *Environ. Sci. Technol.* 57, 4543–4555.
- Liu, M., Siddique, M.S., Graham, N.J.D., Yu, W., 2022b. Removal of small-molecular-weight organic matter by coagulation, adsorption, and oxidation: molecular transformation and disinfection byproduct formation potential. *ACS ES&T Eng.* 2, 886–894.
- Lu, K., Gao, H., Yu, H., Liu, D., Zhu, N., Wan, K., 2022. Insight into variations of DOM fractions in different latitudinal rural black-odor waterbodies of eastern China using fluorescence spectroscopy coupled with structure equation model. *Sci. Total Environ.* 816, 151531.
- Lu, S., Liu, J., Li, S., Biney, E., 2013. Analysis of up-flow aerated biological activated carbon filter technology in drinking water treatment. *Environ. Technol.* 34, 2345–2351.
- Lu, Z., Sun, W., Li, C., Cao, W., Jing, Z., Li, S., Ao, X., Chen, C., Liu, S., 2020. Effect of granular activated carbon pore-size distribution on biological activated carbon filter performance. *Water Res.* 177, 115768.
- Mengjie Liu, N.J.D.G., Xu, Lei, Zhang, Kai, Yu, Wenzheng, 2023. Bubbleless air shapes biofilms and facilitates natural organic matter transformation in biological activated carbon. *Environ. Sci. Technol.* XX:XXXX–XXXX.
- Munz, M., Oswald, S.E., Schäfferling, R., Lensing, H.-J., 2019. Temperature-dependent redox zonation, nitrate removal and attenuation of organic micropollutants during bank filtration. *Water Res.* 162, 225–235.
- Murphy, K.R., Ruiz, G.M., Dunsuir, W.T.M., Waite, T.D., 2006. Optimized parameters for fluorescence-based verification of ballast water exchange by ships. *Environ. Sci. Technol.* 40, 2357–2362.
- Murphy, K.R., Stedmon, C.A., Wenig, P., Bro, R., 2014. OpenFluor— an online spectral library of auto-fluorescence by organic compounds in the environment. *Analytical Methods* 6, 658–661.
- Newton, R.J., Jones, S.E., Eiler, A., McMahon, K.D., Bertilsson, S., 2011. A guide to the natural history of freshwater lake bacteria. *Microbiol. Molecul. Biol. Rev.* 75, 14–49.
- Oksanen J.S.G., Blanchet F., Kindt R., Legendre P., Minchin P.S.P., O'Hara R., Stevens M., Szoecs E., Wagner H., Barbour M.B.B., Bedward M., Borcard D., Carvalho G., Chirico M., De Caceres M.E.H., Durand S., FitzJohn R., Friendly M., Furneaux B., Hannigan, H.M.G., Lahti L., McGlinn D., Ouellette M., Ribeiro Cunha E., Smith T.T.B.C., Stier A., Weedon J. 2022. Vegan: community Ecology Package (R package version 2.6-2).
- Park, M., Snyder, S.A., 2018. Sample handling and data processing for fluorescent excitation-emission matrix (EEM) of dissolved organic matter (DOM). *Chemosphere* 193, 530–537.
- Phungsai, P., Kurisu, F., Kasuga, I., Furumai, H., 2018. Changes in dissolved organic matter composition and disinfection byproduct precursors in advanced drinking water treatment processes. *Environ. Sci. Technol.* 52, 3392–3401.
- Phungsai, P., Kurisu, F., Kasuga, I., Furumai, H., 2019. Molecular characteristics of dissolved organic matter transformed by O₃ and O₃/H₂O₂ treatments and the effects on formation of unknown disinfection by-products. *Water Res.* 159, 214–222.
- Pucher, M., U. Wünsch, G. Weigelhofer, K. Murphy, T. Hein, and D. Graeber. 2019. staRdom: versatile software for analyzing spectroscopic data of dissolved organic matter in R. 11:2366.
- Rattier, M., Reungoat, J., Gernjak, W., Joss, A., Keller, J., 2012. Investigating the role of adsorption and biodegradation in the removal of organic micropollutants during biological activated carbon filtration of treated wastewater. *J. Water Reuse Desalinat.* 2, 127–139.
- Retelletti Brogi, S., Ha, S.-Y., Kim, K., Derrien, M., Lee, Y.K., Hur, J., 2018. Optical and molecular characterization of dissolved organic matter (DOM) in the Arctic ice core and the underlying seawater (Cambridge Bay, Canada): implication for increased autochthonous DOM during ice melting. *Sci. Total Environ.* 627, 802–811.
- Reungoat, J., Escher, B.I., Macova, M., Keller, J., 2011. Biofiltration of wastewater treatment plant effluent: effective removal of pharmaceuticals and personal care products and reduction of toxicity. *Water Res.* 45, 2751–2762.
- Rudolf von Rohr, M., Hering, J.G., Kohler, H.-P.E., von Gunten, U., 2014. Column studies to assess the effects of climate variables on redox processes during riverbank filtration. *Water Res.* 61, 263–275.
- Rui, M., Chen, H., Ye, Y., Deng, H., Wang, H., 2020. Effect of Flow Configuration on Nitrifiers in Biological Activated Carbon Filters for Potable Water Production. *Environ. Sci. Technol.* 54, 14646–14655.
- Sauter, D., Steuer, A., Wasmund, K., Hausmann, B., Szewzyk, U., Sperlich, A., Gniirs, R., Cooper, M., Wintgens, T., 2023. Microbial communities and processes in biofilters for post-treatment of ozonated wastewater treatment plant effluent. *Sci. Total Environ.* 856, 159265.
- Scheili, A., Rodriguez, M.J., Sadiq, R., 2015. Seasonal and spatial variations of source and drinking water quality in small municipal systems of two Canadian regions. *Sci. Total Environ.* 508, 514–524.
- Šimek, K., Horňák, K., Ježbera, J., Nedoma, J., Vrba, J., Straškrábová, V., Macek, M., Dolan, J.R., Hahn, M.W., 2006. Maximum growth rates and possible life strategies of different bacterioplankton groups in relation to phosphorus availability in a freshwater reservoir. *Environ. Microbiol.* 8, 1613–1624.
- Song, W., Z. Gao, M. Hu, X. Wu, Y. Jia, X. Li, Y. Hu, and L. Liao. 2020. Development and technology of rural drinking water supply in China*. 69:187–198.
- Sundaram, V., Pagilla, K., Guarin, T., Li, L., Marfil-Vega, R., Bukhari, Z., 2020. Extended field investigations of ozone-biofiltration advanced water treatment for potable reuse. *Water Res.* 172, 115513.
- Team, R.C., 2022. R: A language and Environment For Statistical Computing. R Foundation for Statistical Computing, Vienna, Austria.
- UNGA. 2001. Road map towards the implementation of the United Nations Millennium Declaration.
- Von Sonntag, C., Von Gunten, U., 2012. Chemistry of Ozone in Water and Wastewater Treatment: From Basic Principles to Applications. IWA Publishing.
- Wan, K., Guo, L., Ye, C., Zhu, J., Zhang, M., Yu, X., 2021. Accumulation of antibiotic resistance genes in full-scale drinking water biological activated carbon (BAC) filters during backwash cycles. *Water Res.* 190, 116744.
- Wang, H., Zheng, Y., Zhu, B., Zhao, F., 2021a. In situ role of extracellular polymeric substances in microbial electron transfer by *Methylomonas* sp. LW13. *Fundamental Res.* 1, 735–741.
- Wang, T., Sun, D., Zhang, Q., Zhang, Z., 2021b. China's drinking water sanitation from 2007 to 2018: a systematic review. *Sci. Total Environ.* 757, 143923.
- WHO. 2023. State of the world's drinking-water: executive summary.
- Xu, L., Campos, L.C., Li, J., Karu, K., Cric, L., 2021a. Removal of antibiotics in sand, GAC, GAC sandwich and anthracite/sand biofiltration systems. *Chemosphere* 275, 130004.
- Xu, L., Zhou, Z., Graham, N.J.D., Liu, M., Yu, W., 2021b. Enhancing ultrafiltration performance by gravity-driven up-flow slow biofilter pre-treatment to remove natural organic matters and biopolymer foulants. *Water Res.* 195, 117010.
- Zhang, B., Shan, C., Wang, S., Fang, Z., Pan, B., 2021. Unveiling the transformation of dissolved organic matter during ozonation of municipal secondary effluent based on FT-ICR-MS and spectral analysis. *Water Res.* 188, 116484.
- Zhang, H., Zhang, Y., Shi, Q., Ren, S., Yu, J., Ji, F., Luo, W., Yang, M., 2012. Characterization of low molecular weight dissolved natural organic matter along the treatment trait of a waterworks using Fourier transform ion cyclotron resonance mass spectrometry. *Water Res.* 46, 5197–5204.
- Zhang, Z., Xi, H., Yu, Y., Wu, C., Yang, Y., Guo, Z., Zhou, Y., 2022. Coupling of membrane-based bubbleless micro-aeration for 2,4-dinitrophenol degradation in a hydrolysis acidification reactor. *Water Res.* 212, 118119.
- Zhao, J., Fang, S., Liu, G., Qi, W., Bai, Y., Liu, H., Qu, J., 2022. Role of ammonia-oxidizing microorganisms in the removal of organic micropollutants during simulated riverbank filtration. *Water Res.* 226, 119250.
- Zheng, X., Ernst, M., Jekel, M., 2010. Pilot-scale investigation on the removal of organic foulants in secondary effluent by slow sand filtration prior to ultrafiltration. *Water Res.* 44, 3203–3213.